

Spectroscopic Study of the $^{24}\text{Mg}^{35}\text{Cl}$ and $^{24}\text{Mg}^{37}\text{Cl}$ $\text{A}^2\Pi\text{-X}^2\Sigma^+$ Band System

R. F. Gutterres, Roberto Ferreira dos Santos, and C. E. Fellows

*Laboratório de Espectroscopia e Laser, Instituto de Física,
Universidade Federal Fluminense, Campus da Boa Viagem, Niterói, RJ 24210-340, Brazil*

Received on 14 July, 2003

The $\text{A}^2\Pi\text{-X}^2\Sigma^+$ emission band system of the MgCl molecule has been studied by means of high resolution Fourier Transform Spectroscopy (FTS). The MgCl species were produced by mixing Mg vapor with a gaseous flow of a He/Cl_2 and excited in a "heated" Schüller's type discharge tube. Rovibrational analysis of the 0-0 and 0-1 bands was performed and the values of the vibrational constant ω_e of the ground state and the spin-orbit constants A_0 and A_J of the $\text{A}^2\Pi$ state were determined. For the first time transitions of the isotopic species $^{24}\text{Mg}^{37}\text{Cl}$ could be assigned and included in the analysis presented here.

1 Introduction

Alkaline-earth mono-halides molecules are highly ionic compounds and have nine valence electrons outside closed shells. This particular electronic configuration have attracted the interest of theoretical and experimental spectroscopists. Several ionic bonding models have been developed to represent the electronic structure of these first excited states [1-3] and experimental studies of these molecules have allowed the test of these models.

The electronic transitions involving the ground and the first excited states of the MgCl molecule have been studied [4-13] from different experiments. Spectroscopic data of the ground state ($v=0, 1$) was also available from accurate microwave experiments [14-16] for several isotopic species of the MgCl molecule. Nevertheless, the limited resolution of the optical experiments did not permit the direct observation of the spin-doubling splitting in the 0-0 band, nor assignments for the isotopic molecule $^{24}\text{Mg}^{37}\text{Cl}$ transitions, of the $\text{A}^2\Pi\text{-X}^2\Sigma^+$ system.

It was only recently that the $\text{A}^2\Pi\text{-X}^2\Sigma^+$ system could be studied by means of the high resolution Fourier Transform Spectroscopy. The emission spectra was produced in Orsay and Waterloo by using different techniques, and the strong similarity of the obtained spectra have allowed a joint analysis [17]. A complete rovibrational analysis of the $\text{A}^2\Pi\text{-X}^2\Sigma^+$ 0-0 and 0-1 bands, including vibrational dependence of the ground state and spin-orbit splitting of the $\text{A}^2\Pi$ state, was carried out. The obtained value of the lambda doubling constant p was found positive, in contrast with the theoretical predictions [18].

This work presents a complementary analysis of the data obtained earlier [17]. For the first time 56 transitions of the $^{24}\text{Mg}^{37}\text{Cl}$ $\text{A}^2\Pi\text{-X}^2\Sigma^+$ 0-0 band could be assigned. A set of molecular constants, which reproduce the observed transi-

tions of both $^{24}\text{Mg}^{35}\text{Cl}$ and $^{24}\text{Mg}^{37}\text{Cl}$ compounds, could be derived from a nonlinear least-squares fit of the optical data obtained from the Orsay group measurements.

2 The experiment

Excited MgCl species were produced in a Schüller's type tube which was heated in its middle part. More details of Schüller discharge device can be found elsewhere [19]. Briefly this discharge tube consists of a quartz tube for which both electrodes are located in front of a liquid nitrogen trap. In this way, electrodes are preventing of any contamination, resulting in a very stable discharge intensity. This light source is particularly convenient for emission Fourier Transform Spectroscopy. The MgCl molecules were produced in the following way: Mg pellets were introduced in the middle part of the discharge tube which was heated up to 800°C , in order to obtain Mg vapor. The DC discharge (3400 V, 100 mA) was established through flowing He/Cl_2 gas mixture (1% of Cl_2 in He), at a pressure of 30 mbar. The spectrum was recorded by means of a Bruker IFS 120 HR Fourier Transform Spectrometer. The detector was a photo-multiplier tube (HAMAMATSU 1P28) associated with a long pass wavelength colored glass filter. The spectrum was obtained after the transformation of 1000 co-added interferograms recorded at an apodized resolution of 0.060 cm^{-1} .

3 Results

The observed high line density given by overlapping branches of this emission spectrum is a consequence of both the doublet structure of the involved electronic states and the

very similar potential curve of the upper and lower states. In a $A^2\Pi-X^2\Sigma^+$ electronic transition one can expect to observe twelve branches for each band [20]. In addition these electronic states which have similar vibrational (and rotational) constants, result in sequences in which the separations of the bands are about 30 cm^{-1} .

An overview of a part of the obtained spectrum is shown in the Fig. 1. The $A^2\Pi-X^2\Sigma^+$ 0-0 band can be clearly seen in this figure, which shows the band head of the branches P_{12} , P_{11} , P_{22} , Q_{22} . Only transitions of the 0-1 $A^2\Pi_{1/2}-X^2\Sigma^+$ could be assigned in the sequence $\Delta v = -1$.

Rotational structure of the P_{12} branches for both the $^{24}\text{Mg}^{35}\text{Cl}$ and the $^{24}\text{Mg}^{37}\text{Cl}$ isotopic species are shown in the Fig. 2. A total of 493 transitions was assigned, including 56 transitions of the not-predominant $^{24}\text{Mg}^{37}\text{Cl}$ isotopic species. These 56 transitions were assigned in the P_{12} , Q_{11} and R_{22} branches of the 0-0 band.

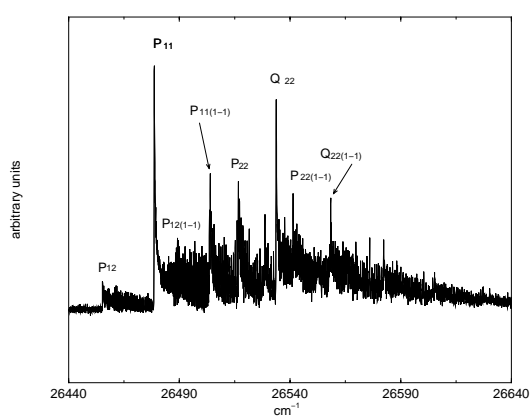


Figure 1. Overview of the A-X spectrum.

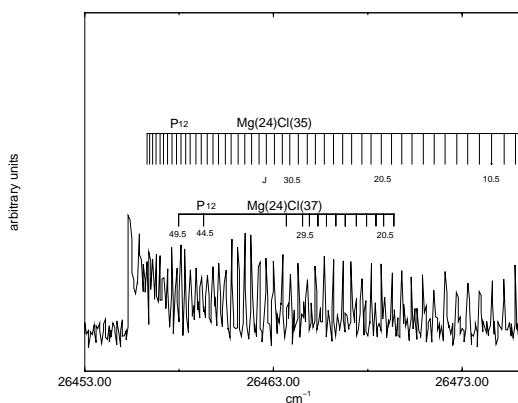


Figure 2. Part of P_{12} branch of the 0-0 A-X sub-band.

4 Analysis

Figure 3 shows a Fortrat diagram of the assigned transitions. This data set was analyzed in two different ways. In the first approach, the molecular constants were derived by adjusting all obtained data concerning both the 0-0 and 0-1 bands. In the second approach, the assigned lines of each band system were treated separately. In both analysis procedures, it was also possible to test the quality of the assignments taking into account the molecular constants of the ground state obtained from micro-wave experiments [14, 15]. It was expected that the molecular constants calculated in this work should have a high coherence and complementarity with the very accurate constants derived in [14, 15].

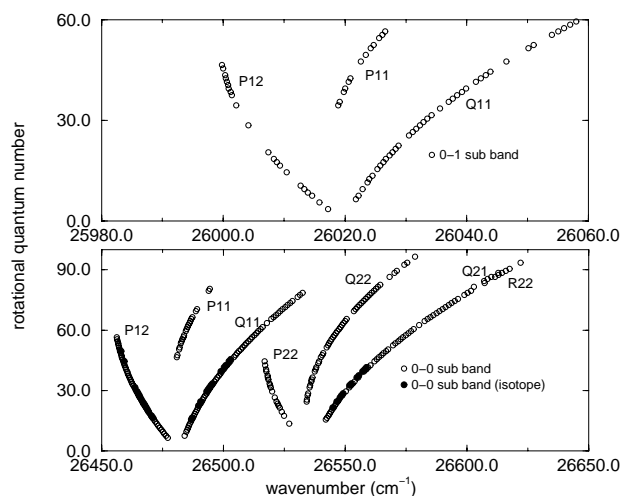


Figure 3. Fortrat diagram of the A-X band system. The points represented by open circles (\circ) are the observed energy levels and correspondent wavenumbers of the $^{24}\text{Mg}^{35}\text{Cl}$ species, the full circles (\bullet) are the observed energy levels and correspondent wavenumbers of the $^{24}\text{Mg}^{37}\text{Cl}$ species.

4.1 The Hamiltonian representation

The spectroscopic constants for the $A^2\Pi$ and $X^2\Sigma^+$ electronic states were determined by a nonlinear least-squares fit of all observed wavenumbers. The energy term values of the $X^2\Sigma^+$ electronic state were described by a standard Hund's case "b" $^2\Sigma^+$ formulae,

$$\begin{aligned}
T &= T_v + B_v N(N+1) - D_v [N(N+1)]^2 + \\
&+ H_v [N(N+1)]^3 + \dots + \\
+\frac{1}{2} \gamma & N \text{ for } e \text{ labelled } F_1 \text{ levels, and} \\
-\frac{1}{2} \gamma & (N+1) \text{ for } f \text{ labelled } F_2 \text{ levels, with:} \\
T_v &= T_e + \omega_e(v+1/2) - \omega_e x_e(v+1/2)^2 + \omega_e y_e(v+1/2)^3 + \dots \\
B_v &= B_e - \alpha_B(v+1/2) + \beta_B(v+1/2)^2 + \dots \\
D_v &= D_e + \alpha_D(v+1/2) + \dots \\
\gamma &= \gamma_e + \gamma_v(v+1/2) + \gamma_D N(N+1) + \dots
\end{aligned} \tag{1}$$

The Hamiltonian for the isolated A²Π electronic state is shown in Table 1. The observed transitions involve only one vibrational level ($v = 0$) of the A²Π state, consequently no vibrational dependence was taken into account in the Hamiltonian representation of this state. The data from the ²⁴Mg³⁷Cl molecule were included in the fit using standard transformation formulae [21]. An additional parameter ϵ

was considered in the reductions. It was defined for the isotopic species as a slight change in the origin of the energies T ,

$$T_{isot} = T + (1 - \rho)\epsilon, \tag{2}$$

ρ being the square root of the ratio between the reduced masses of ²⁴Mg³⁵Cl and ²⁴Mg³⁷Cl species, respectively.

Table 1. Hamiltonian energy matrix for the A²Π electronic state.

	² Π _{3/2}	² Π _{1/2}
² Π _{3/2}	$ \begin{aligned} &T + A/2 + (B + A_J)(X - 1) \\ &- D[(X - 1)^2 + X] \\ &+ H[(X - 1)^3 + X(3X - 1)] \\ &+ (A_{JJ}/2)[3(X - 1)^2 + X] + (q/2)X \end{aligned} $	$ \begin{aligned} &- BX^{1/2} + 2DX^{3/2} \\ &- HX^{1/2}(3X^2 + X + 1) + A_{JJ}X^{1/2} \\ &+ (q/2)[X^{1/2}[-1 \pm (X + 1)^{1/2}]] \\ &- (p/4)X^{1/2} \end{aligned} $
² Π _{1/2}	sym.	$ \begin{aligned} &T - A/2 + (B + A_J)(X - 1) \\ &- D[(X + 1)^2 + X] \\ &+ H[(X + 1)^3 + X(3X + 1)] \\ &- (A_{JJ}/2)[3(X + 1)^2 + X] \\ &+ (q/2)[X + 2 \mp 2(X + 1)^{1/2}] \\ &+ (p/2)[1 \mp (X + 1)^{1/2}] \end{aligned} $

Note. $X = (J + 1/2)^2 - 1$. The \pm signs refer to the levels with ef parity respectively.

4.2 The first approach: global reduction of the analysis data set

It appeared that no local perturbation affects the spectrum and, consequently a merged fit involving all observed transitions for the ²⁴Mg³⁵Cl and ²⁴Mg³⁷Cl isotopic species was performed in this work. A set of 14 molecular constants was derived, reproducing the observed transitions with a standard deviation less than $1.5 \times 10^{-2} \text{ cm}^{-1}$. Tables 2(a) and 3(a) show the molecular constants issued from these calculations for the X²Σ⁺ and A²Π states, respectively.

As a second global analysis procedure, a new adjust of

the obtained global data set was performed, in which the ground state molecular constants $B_e, \alpha_B, \beta_B, \gamma_e, \gamma_v$ and γ_B were held fixed in the values calculated by M. Bogey *et al.* [14]. The molecular constant values obtained by Bogey *et al.* [14] were used, instead of those obtained by Ohshima and Endo [15], because these parameters were derived in a data reduction merging all vibrational observed levels ($v = 0, 1$ and 2), allowing, therefore, a more adequate comparison between the results presented in this sub-section. All adjustable parameters of the A²Π state, as well as the parameter ω_e of the ground state, were left free in this new global data reduction. From this second procedure a set of

10 parameters was determined and no significant change in the r.m.s. of the adjust could be observed.

Table 2. Molecular constants in cm^{-1} for the $X^2\Sigma^+$ electronic state determined in the analysis from a nonlinear least-squares fit of the global data set. Column (b) shows, for comparison, the values obtained by Bogey *et al.* [14]. Numbers in parentheses represent the standard deviation in units of the last figure quoted.

coeff.	$X^2\Sigma^+(a)$	$X^2\Sigma^+(b)$
T_e^\dagger	[0]	-
B_e	0.2455751(250)	0.2456153684(43)
$D_e \times 10^{+7}$	2.6897(357)	2.723173(50)
$\alpha_B \times 10^{+3}$	1.60231(194)	1.6203910(53)
$\beta_B \times 10^{+6}$	-	3.5958(53)
ω_e	462.09051(342)	462.10614(298) [‡]
$\gamma_e \times 10^{+2}$	0.21294(975)	0.223271(19)
$\gamma_v \times 10^{+5}$	-	-2.9053(73)
$\gamma_D \times 10^{+8}$	-	-0.743(20)

[†] Origin of the energies at level $v = -1/2$.

[‡] Value obtained by fixing the ground state molecular constants in the values obtained in [14] (see text).

$N = 0$ of the ground state ($T_e = 0$).

(a) This work, (b) M. Bogey *et al.* [14]

Table 3. Molecular constants in cm^{-1} for the $A^2\Pi$ electronic state determined in the analysis from (a) the nonlinear least-squares fit of the global data set, (b) values obtained by fixing the molecular constants of the ground state in the ones obtained in [14] (see text). Numbers in parentheses represent the standard deviation in units of the last figure quoted.

coeff.	$A^2\Pi(a)$	$A^2\Pi(b)$
T_0^\dagger	26740.14163(331)	26740.15355(276)
B_0	0.2507822(298)	0.25081495(147)
$D_0 \times 10^{+7}$	2.5689(466)	2.64642(195)
ϵ^\dagger	-242.960(242)	-243.131(252)
A_0	54.7850(427)	54.7978(342)
$A_J \times 10^{+4}$	-0.4854(171)	-0.5023(143)
$p_0 \times 10^{+2}$	0.5159(114)	0.52860(716)
$q_0 \times 10^{+4}$	-0.2331(189)	-0.1994(102)

[†] Origin of the energies at level $v = -1/2$,

$N = 0$ of the ground state ($T_e = 0$).

[‡] $\Delta\nu_{fe} = p_0 \times (J + 1/2)$.

The values of the molecular constants for the ground state obtained by M. Bogey *et al.* [14], as well as the ω_e value calculated in the procedure described above, are shown in Table 2 (column b). A strong coherence between the values listed in both Table 2 (column a) and Table 2 (column b) can be observed. The calculated molecular constants of the $A^2\Pi$ excited state, obtained in the second analysis procedure described above, are shown in Table 3 (column b). Again a very good agreement between the molecular constant values shown in Table 3 (column a) and the ones shown in Table 3 (column b) can be noted.

4.3 The second approach: the independent reduction 0-0 and 0-1 band system data set

The data sets of the 0-0 and the 0-1 band systems were analyzed also separately. At first the 0-0 band was analyzed using the Hamiltonian described in the Section 4.1, in which the vibrational dependence was not taken into account. A set of 11 molecular constants was derived and it reproduced the observed transitions of the 0-0 band system within a standard deviation around $1.5 \times 10^{-2} \text{ cm}^{-1}$.

In the analysis involving the data of the 0-1 band system only transitions involving the $A^2\Pi_{1/2}-X^2\Sigma^+$ sub-band could be assigned. The spin orbit parameters A_0 and A_J were therefore held fixed in the value obtained from the analysis of the 0-0 band system. Also no lines concerning the $^{24}\text{Mg}^{37}\text{Cl}$ isotopic species were assigned in this band system. A set of 6 molecular constants was obtained in the data reduction, which reproduced the observed transitions of the 0-1 band system within a standard deviation around $1.5 \times 10^{-2} \text{ cm}^{-1}$. Tables 4(a) and 5(a) show the molecular constants for the $X^2\Sigma^+$ and $A^2\Pi$ states respectively, issued from the calculations for each band system.

In an analogous analysis procedure described in the Section 4.2, a new adjust of the 0-0 and the 0-1 band system data was performed, in which the ground state molecular constants B_v , D_v , γ_v and γ_{D_v} were held fixed in the values obtained by Ohshima and Endo [15]. In this case, the choice of the molecular constants calculated in [15] instead of those calculated by Bogey *et al.* [14], is due to the fact that in the work of Ohshima and Endo each vibrational level ($v = 0$ and 1) has been fitted separately, allowing a more adequate comparison between the results presented in this sub-section. All adjustable parameters of the $A^2\Pi$ state were left free in the adjust involving the 0-0 band system data set while those of the ground state were held fixed to the values reported in [15] for $v''=0$. From this second procedure a set of 10 parameters was calculated and no significant change in the r.m.s. of the adjust could be observed.

Also the 0-1 band system was analyzed by fixing the molecular constants B_v , D_v , γ_v and γ_{D_v} of the ground state in the values obtained by Ohshima and Endo [15] for $v'' = 1$, and leaving the adjustable molecular constants of the $A^2\Pi$ state as free parameters. A new set of 4 parameters, for the $A^2\Pi$ state, was calculated from this procedure. No significant change in the r.m.s. of the adjust was observed.

The molecular constant values for the ground state obtained in [15] for $v = 0$ and $v = 1$ are shown in the Table 4(b). A reasonable agreement between the values listed in both Table 4(a) and Table 4(b) is observed. The calculated molecular constants of the $A^2\Pi$ excited state, obtained in the 0-0 and 0-1 sub band analyses described above, are shown in Table 5(b). Once more a very good agreement between the molecular constant values calculated for the $A^2\Pi$ state, shown in Tables 5(a) and Table 5(b), can be noted. Furthermore, Tables 4(c) and 5(c) show the values of the molecular

constants obtained by M. Singh *et al.* [10] for both states. The differences between the obtained constants and the ones obtained in [10] are, to some extent, a consequence of different Hamiltonians used to represent the energy levels of

the $X^2\Sigma^+$ and $A^2\Pi$ states. In the analysis of M. Singh *et al.* [10] no spin-orbit value determination, nor the $^{24}\text{Mg}^{37}\text{Cl}$ isotopic species transitions were included.

Table 4. Molecular constants in cm^{-1} for the $X^2\Sigma^+$ electronic state determined in the analysis from a nonlinear least-squares fit of the 0-0 and 0-1 band system data sets. Column (b) shows, for comparison, the values obtained by Ohshima and Endo [15]. Numbers in parentheses represent the standard deviation in units of the last figure quoted.

(v=0)	$X^2\Sigma^+$ (a)	$X^2\Sigma^+$ (b)	$X^2\Sigma^+$ (c)
B	0.2447159(265)	0.2448806155(30)	0.244664(37)
$D \times 10^{+7}$	2.6130(505)	2.724584(47)	2.682(79)
$\gamma \times 10^{+2}$	0.19933(795)	0.22197690(80)	0.17 [†]
$\gamma_D \times 10^{+9}$	-	-9.373(80)	-
(v=1)	$X^2\Sigma^+$ (a)	$X^2\Sigma^+$ (b)	$X^2\Sigma^+$ (c)
B	0.242522(103)	0.2431928258(37)	0.243051(37)
$D \times 10^{+7}$	2.351(309)	2.721816(70)	2.704(80)
$\gamma \times 10^{+2}$	-	0.2189581(23)	0.17 [†]
$\gamma_D \times 10^{+9}$	-	-8.37(10)	-

[†] Approximated values.

Table 5. Molecular constants in cm^{-1} for the $A^2\Pi$ electronic state determined in the analysis from: (a) the nonlinear least-squares fit of the 0-0 and 0-1 band system data sets, (b) values obtained by fixing the molecular constants of the ground state in this ones obtained in [15](see text), (c) values obtained by Singh *et al.* [10]. Numbers in parentheses represent the standard deviation in units of the last figure quoted.

0-0 band sys.	$A^2\Pi$ (a)	$A^2\Pi$ (b)	$A^2\Pi$ (c)
T_0^\dagger	26509.09672(210)	26509.10012(276)	26481.927(8) ($A^2\Pi_{1/2}$) 26535.865(5) ($A^2\Pi_{3/2}$)
B_0	0.2507297(259)	0.25089302(150)	0.251813(74) ($A^2\Pi_{1/2}$) 0.249521(74) ($A^2\Pi_{3/2}$)
$D_0 \times 10^{+7}$	2.5414(500)	2.65089(195)	2.389(156) ($A^2\Pi_{1/2}$) 2.818(162) ($A^2\Pi_{3/2}$)
ϵ^\dagger	-126.74(234)	-128.68(246)	-
A_0	54.48413(334)	54.47720(334)	-
$A_J \times 10^{+4}$	-0.4847(166)	-0.5084(131)	-
$p_0 \times 10^{+2}$	0.5231(127)	0.51312(740)	0.55(2) [‡]
$q_0 \times 10^{+4}$	-0.2243(198)	-0.22387(995)	-
0-1 band sys.	$A^2\Pi$ (a)	$A^2\Pi$ (b)	$A^2\Pi$ (c)
T_0^*	26047.00372(439)	26047.01428(407)	26019.811(5) ($A^2\Pi_{1/2}$)
B_0	0.250070(101)	0.25076900(605)	-
$D_0 \times 10^{+7}$	2.154(299)	2.5535(164)	-
$p_0 \times 10^{+2}$	0.6728(162)	0.5612(157)	-

[†] Origin of the energies at level $v = 0$, $N = 0$ of the ground state ($T_0 = 0$).

* Origin of the energies at level $v = 1$, $N = 0$ of the ground state ($T_1 = 0$).

[‡] $\Delta\nu_{fe} = p_0 \times (J + 1/2)$.

5 Conclusion

The $A^2\Pi$ - $X^2\Sigma^+$ band system of the MgCl molecule was studied by means of the Fourier Transform Spectroscopy (FTS). The MgCl molecules were produced by mixing Mg vapor with a gaseous flow of a He/Cl₂, and excited in a heated Schüller type discharge tube. An accurate set of

molecular constants was determined from a complete rovibrational analysis of the 0-0 and 0-1 bands, including vibrational dependence on the ground state and spin-orbit splitting of the $A^2\Pi$ state, and also by an independent 0-0 and 0-1 band system analysis. In both analysis procedures it was possible to take into account the molecular constants previously obtained [14, 15] for the ground state, which

were calculated with high accuracy. The high resolution of the FTS technique allows for the first time the observation and assignment of the $^{24}\text{Mg}^{37}\text{Cl}$ isotopic species transitions, which were included in the analysis presented in this work.

Acknowledgements

This work was partially supported by CAPES/COFECUB (Brazil/France cooperation) 182/96. One of the authors (C.E.F.) would like to thank CAPES/Brasil for a post-doctoral grant.

References

- [1] T. Törring W. E. Ernst, and S. Kindt, *J. Chem. Phys.* **90**, 4927 (1989).
- [2] T. Törring W. E. Ernst, and J. Kändler, *J. Chem. Phys.* **81**, 4614 (1984).
- [3] S. F. Rice, H. Martin, and R. W. Field, *J. Chem. Phys.* **82**, 5023 (1985).
- [4] K. P. Huber and G. Herzberg, *Molecular spectra and molecular structure: Constants of diatomic molecules.*, Vol. 4, Van Nostrand Reinhold Co., New York, NY. 1979.
- [5] F. Morgan, *Phys. Rev.* **50**, 603 (1936).
- [6] V. S. N Rao, and P. T. Rao, *Indian J. Phys.* **37**, 640 (1963).
- [7] A. B. Darji, N. R. Shah, P. M. Shah, M. B. Sureshkumar, and G. S. Desai, *Pramana* **25**, 571 (1985).
- [8] E. Morgan, R. F. Barrow, *Nature(London)* **192**, 1182 (1961).
- [9] M. M. Patel and P. D. Patel, *Indian J. Phys.* **42**, 254 (1968).
- [10] M. Singh, G. S. Ghodgaokar, and M. D. Saksena, *Can. J. Phys.* **65**, 1594 (1987).
- [11] M. Singh, M. D. Saksena, and G. S. Ghodgaokar, *Can. J. Phys.* **66**, 570 (1988).
- [12] B. Bourguignon, Mohammed-Ali Gargoura, J. Rostas, and G. Taieb, *J. Phys. Chemistry.* **91**, 2080 (1987).
- [13] J. Rostas, N. Shafizadeh, G. Taieb, B. Bourguignon, and M. G. Prisant, *Chem. Phys.* **142**, 97 (1990).
- [14] M. Bogey, C. Demuyne, and J. L. Destombes, *Chem. Phys. Lett.* **155**, 265 (1989).
- [15] Y. Ohshima and Y. Endo, *Chem. Phys. Lett.* **213**, 95 (1993).
- [16] M. A. Anderson, and L. M. Ziurys, *Chem. Phys. Lett.* **224**, 381 (1994).
- [17] T. Hirao, P. F. Bernath, C. E. Fellows, R. F. Gutterres, M. Vervloet, *J. of Molec. Spectrosc.* **212**, 53 (2002).
- [18] H. Lefebvre-Brion and R. W. Field, *Perturbation in the Spectra of Diatomic Molecules*, Academic Press, 1986.
- [19] J. H. Callomon, *Can. J. Phys.* **34**, 1046 (1956).
- [20] G. Herzberg, *Molecular spectra and molecular structure: I. Spectra of diatomic molecules.*, Van Nostrand Reinhold Co., New York, NY. 1950.
- [21] C. Ryzlewicz, H. U. Schütze-Pahlmann, J. Hoefl, and T. Törring, *Chem. Phys.* **71**, 389 (1982).